

Simulation of Water Entry of a Free-falling Wedge by Improved MPS Method

*Youlin Zhang, Zhenyuan Tang, Decheng Wan**

State Key Laboratory of Ocean Engineering, School of Naval Architecture, Ocean and Civil Engineering, Shanghai Jiao Tong University,
Collaborative Innovation Center for Advanced Ship and Deep-Sea Exploration, Shanghai, China

*Corresponding author

ABSTRACT

In the present study, the process of free-falling wedge impacting on water is numerically studied by our in house solver based on Moving Particle Semi-Implicit (MPS) method. Some improved schemes are used in this solver to suppress numerically unphysical pressure oscillation in traditional MPS method. For validation purpose, computational results of wedge with different tilting angles are compared against experimental results from the Wave Induced Loads on Ships Joint Industry Project III (WILS JIP-III). Numerical pressures, free surface elevations and velocities of wedge show agreement with experimental data.

KEY WORDS: Particle method; MPS (moving particle semi-implicit); wedge; free-falling; water-entry; slamming.

INTRODUCTION

During ship sailing at rough sea, slamming occurs when the forefoot of ship hull rises above the water surface and then drops into water with high vertical velocity (Southall et al., 2014). Periodical and short duration impact loads can cause serious damage to ship structure. Hence, the slamming problem is important for ship design and operation.

Over the past decades, the slamming problem was commonly investigated as the similar flow of wedge entry into water (Yang and

Qiu, 2012), and firstly studied by von Karman (1929) and Wagner (1932). Among the early established methods, theoretical approaches were much popular to solve this problem. However, these methods are hard to describe the complex nonlinear free surface flow. On the contrary, kinds of numerical methods based on the Navier-Stokes equation are developed and show the capability to solve the water entry problem. Among these approaches, Lagrangian particle methods are more and more popular to free surface flow problems in the near few years. The Smoothed Particle Hydrodynamics (SPH) and Moving Particle Semi-implicit (MPS) methods are the representative Lagrangian type mesh-less methods. The SPH method is originally developed for compressible flows by Monaghan (1994). By choosing a sufficiently high speed of sound and a much small size of time step, it can be employed to solve water entry problem (Oger et al., 2006; Shao 2009; Liu et al., 2012; Koukouvinis et al., 2013; Ma and Liu, 2014; Amicarelli et al., 2015). Compared to SPH method, MPS method was originally proposed by Koshizuka and Oka (1996) for incompressible flow. Since the pressure of fluid is computed by a semi-implicit algorithm, a relatively large size of time step can be used in MPS method. Recently, several applications of the water entry problem based on MPS method were published. For example, Lee et al. (2010) employed the MPS method to calculate the impact loads by falling flat plate with incident angles. Yokoyama et al. (2014) numerically studied the water entry of spheres by MPS method and discussed the influence of the surface conditions of the solids falling into the water on the formation of the splashes. Sun et al. (2015) proposed a MPS and modal superposition coupled method to study the 2D flexible symmetric wedge dropping into water problem. Hwang et al. (2015) developed a

MPS-FEM coupled method to simulate a wet drop with deformable wedge.

However, accuracy of the MPS method is necessary to be improved. Fortunately, lots of approaches are published to suppress the numerically unphysical pressure oscillation in traditional MPS method (Khayyer et al., 2009, 2010, 2011, 2012; Kondo et al., 2011; Lee et al., 2011; Tanaka et al., 2010; Ikari et al., 2015) and avoid falsely detected free surface particles (Zhang et al., 2014). In the present study, a MPS solver MLParticle-SJTU is used for all simulation works. Some improved schemes are used in this solver to suppress numerically unphysical pressure oscillation. These improvements include: (1) modified kernel function (Zhang et al., 2014); (2) momentum conservative pressure gradient model; (3) mixed source term method for Poisson equation of pressure (Tanaka et al., 2010); (4) surface detection method based on asymmetry of neighbor particles. The performance of MLParticle-SJTU has been published by many applications in large free-surface deformation problems, such as dam breaking flow (Zhang, et al., 2011), liquid sloshing in LNG tank (Zhang et al., 2012, 2014), impinging jet flows (Tang et al., 2015), etc.

In this paper, the 2D symmetric and asymmetric wedges dropping problems are numerically studied. Time history of impacting pressures, motions of wedge, deformation and splashes of free surface are presented. According to the comparison between numerical results by the improved MPS method and experimental results from the Wave Induced Loads on Ships Joint Industry Project III (WILS JIP-III) (Kim et al., 2014; Southall et al., 2014), capability and credibility of the MPS solver MLParticle-SJTU about water entry problem is investigated.

NUMERICAL SCHEME

In present section, the improved MPS method is briefly reviewed as below. Details of the method can be found in the previous work (Zhang et al., 2014).

Governing Equations

Governing equations for incompressible viscous fluid are represented as

$$\nabla \cdot \mathbf{V} = 0 \quad (1)$$

$$\frac{D\mathbf{V}}{Dt} = -\frac{1}{\rho} \nabla P + \nu \nabla^2 \mathbf{V} + \mathbf{g} \quad (2)$$

where \mathbf{V} is the velocity vector, t is time, ρ is water density, P is pressure, ν is kinematic viscosity, \mathbf{g} is the gravity acceleration.

Particle Interaction Models

In particle method, governing equations should be replaced by the particle interaction models, include the differential operators of gradient, divergence and Laplacian.

In the present study, an improved gradient operator, proposed by Tanaka (2010), is expressed as

$$\langle \nabla \phi \rangle_i = \frac{D}{n^0} \sum_{j \neq i} \frac{\phi_j + \phi_i}{|\mathbf{r}_j - \mathbf{r}_i|^2} (\mathbf{r}_j - \mathbf{r}_i) \cdot W(|\mathbf{r}_j - \mathbf{r}_i|) \quad (3)$$

where ϕ is an arbitrary scalar function, D is the number of space dimensions, n^0 is the initial particle number density for incompressible flow.

The function $W(r)$ in Eq.(3) is the kernel function which represents the effect between neighboring particles and center particle. In present paper, the improved kernel function, has a similar form with the kernel function proposed by Koshizuka (1996) but without singularity at $r=0$, is defined as

$$W(r) = \begin{cases} \frac{r_e}{0.85r + 0.15r_e} - 1 & 0 \leq r < r_e \\ 0 & r_e \leq r \end{cases} \quad (4)$$

where r is distance between particles, r_e is the effect radius and equal to 2.1 in this paper. The particle number density in MPS method is defined as

$$\langle n \rangle_i = \sum_{j \neq i} W(|\mathbf{r}_j - \mathbf{r}_i|) \quad (5)$$

The divergence operator is expressed as

$$\langle \nabla \cdot \boldsymbol{\Phi} \rangle_i = \frac{D}{n^0} \sum_{j \neq i} \frac{(\boldsymbol{\Phi}_j - \boldsymbol{\Phi}_i) \cdot (\mathbf{r}_j - \mathbf{r}_i)}{|\mathbf{r}_j - \mathbf{r}_i|^2} W(|\mathbf{r}_j - \mathbf{r}_i|) \quad (6)$$

where $\boldsymbol{\Phi}$ is an arbitrary vector.

And the Laplacian operator is expressed as

$$\langle \nabla^2 \phi \rangle_i = \frac{2D}{n^0 \lambda} \sum_{j \neq i} (\phi_j - \phi_i) \cdot W(|\mathbf{r}_j - \mathbf{r}_i|) \quad (7)$$

$$\lambda = \frac{\sum_{j \neq i} W(|\mathbf{r}_j - \mathbf{r}_i|) \cdot |\mathbf{r}_j - \mathbf{r}_i|^2}{\sum_{j \neq i} W(|\mathbf{r}_j - \mathbf{r}_i|)} \quad (8)$$

where λ is a parameter, introduced to keep the variance increase equal to that of the analytical solution.

Model of incompressibility

The time integration algorithm of incompressibility for the improved MPS method is a fractional step algorithm similar to SMAC (Simplified Marker-and-Cell) method. Of which, pressure is implicitly calculated by solving a Poisson equation. According to the work of Tanaka and Masunaga (2010), unphysical oscillation of pressure can be obviously suppressed by the introduction of mixed source term into the Poisson equation, and the improved pressure Poisson equation can be expressed as

$$\langle \nabla^2 P^{n+1} \rangle_i = (1 - \gamma) \frac{\rho}{\Delta t} \nabla \cdot \mathbf{V}_i^* - \gamma \frac{\rho}{\Delta t^2} \frac{\langle n^* \rangle_i - n^0}{n^0} \quad (9)$$

where γ is a blending parameter with a value between 0 and 1. The range of $0.01 \leq \gamma \leq 0.05$ is better according to numerical experiments conducted by Lee et al.(2011). In this paper, $\gamma = 0.01$ for all

simulations. The BiCGSTAB (Biconjugate gradient stabilized) method is employed to solve the PPE.

Free Surface Particle Detection Method

To improve the accuracy of surface particle detection, we employ an improved free surface detection method in which a vector function is defined as follow (Zhang et al., 2014):

$$\langle \mathbf{F} \rangle_i = \frac{D}{n^0} \sum_{j \neq i} \frac{1}{|\mathbf{r}_i - \mathbf{r}_j|} (\mathbf{r}_i - \mathbf{r}_j) W(r_{ij}) \quad (10)$$

The vector function \mathbf{F} represents the asymmetry of arrangements of neighbor particles. It points out of fluid region and has a large amplitude at the free surface, but equals to zero for particles with symmetrical neighboring particles.

For a surface particle, the following equation should be satisfied

$$\langle \mathbf{F} \rangle_i > \alpha \quad (11)$$

where α is a parameter, and has a value of $0.9 |\mathbf{F}|^0$ in this paper, $|\mathbf{F}|^0$ is the initial value of $|\mathbf{F}|$ for surface particle.

Motion of free-falling wedge

The wedge is free to move in vertical direction but restrained in other freedoms. The motion of the wedge is governed by the equation of rigid body dynamics, following the Newton's law of motion.

$$M \frac{d\mathbf{V}_G}{dt} = M\mathbf{g} + \mathbf{F}_{fluid-solid} \quad (12)$$

where M is the mass of the wedge, \mathbf{V}_G is the linear velocity of the center of gravity, $\mathbf{F}_{fluid-solid}$ is the hydrodynamic force acting on the body.

COMPUTATIONAL SETUP

In order to validate the capability and credibility of the MPS solver MParticle-SJTU for water entry problems, both symmetric and asymmetric wedge free dropping tests are numerically studied and compared against experimental data proposed by MOERI as part of the WILS JIP-III. Computational domain is set with similar geometrical size with the experiment, and shown as Fig.1. Details of the model and pressure sensors arrangement are shown as Fig.2. The wedge is initially mounted upon the calm water surface with the distance of 0.5m. Dead-rise angle of the wedge is 30deg. The tilting angle varies for symmetric and asymmetric wedge drop tests, as shown in Table 1.

Table 1. Parameters of wedge drop tests

Cases	Dead-rise angle (deg)	Tilting angle (deg)	Drop height (m)
Case1	30	0	0.5
Case2	30	10	0.5
Case3	30	20	0.5

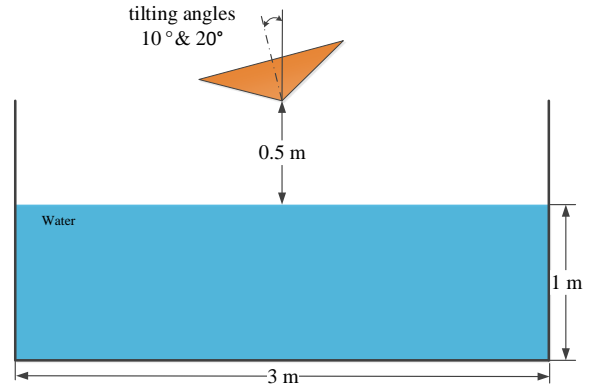


Fig.1 Computational setup

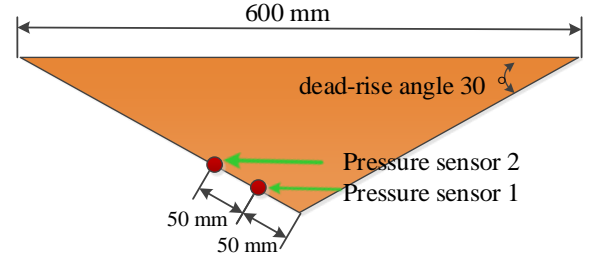


Fig.2 Model and pressure sensors arrangement

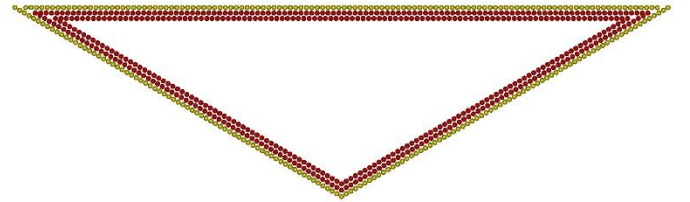


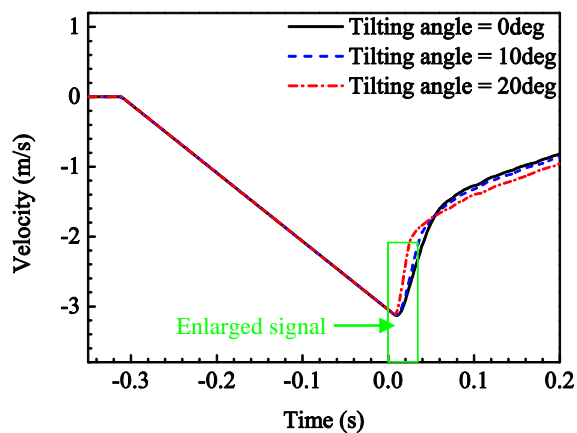
Fig.3 Particle arrangement to make the wedge

In this paper, both wedge and fluid domain is dispersed by particles. The wedge is composed by particles which are arranged around outline of the wedge uniformly, as shown in Fig.3. Computational conditions are same except variety of tilting angles of the wedge for all cases. The initial particle spacing is 0.005m. The total number of particles is 124745, and 119800 fluid particles included. The gravitational acceleration and water density are 9.8m/s^2 and 1000kg/m^3 , respectively. The kinematic viscosity of water is given by $1.01 \times 10^{-6} \text{m}^2/\text{s}$. The time step size is 0.0005s.

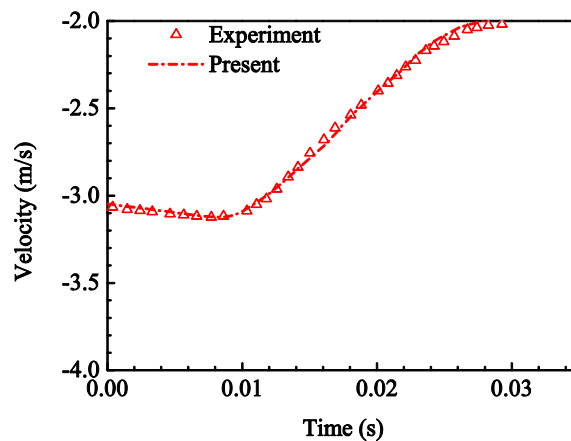
NUMERICAL RESULTS

Time histories of velocities

The comparison of drop velocities is shown as Fig.4. The time of initial entry of wedge is adjusted to $t=0.0\text{s}$. According to Fig.4 (a), it takes 0.319s for the wedge freely falling to the water surface. Then, velocities of the wedge decrease due to the impact loads in the opposite direction of motion. Since velocities and impact loads vary rapidly within 0.035 s, velocity signals of the wedge with different tilting angles are enlarged and shown as Fig.4 (b~d). The maximum numerical velocity is 3.13 m/s which is the ideal value corresponding to the drop height of 0.5 m. With the increasing of tilting angles, motions of the wedge decelerated more fleetly. Moreover, time histories of velocities are all in good agreement with experimental results of the WILS JIP-III.

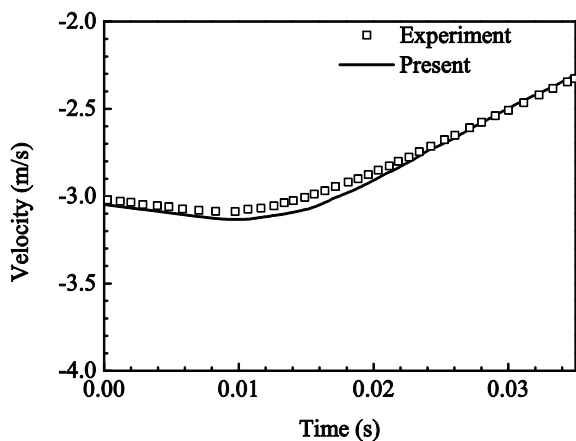


(a) Total signal

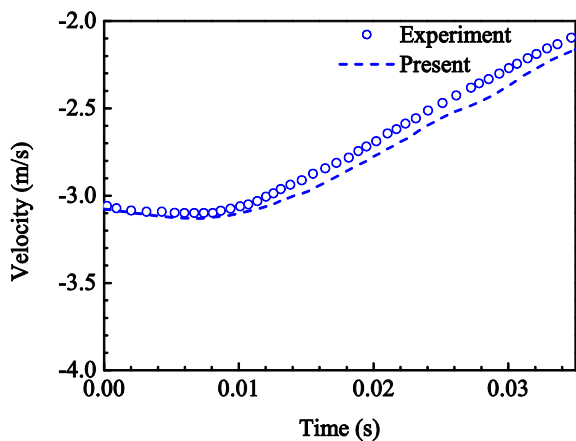


(d) Enlarged signal (20deg tilt)

Fig.4 Comparison of drop velocity



(b) Enlarged signal (0deg tilt)



(c) Enlarged signal (10deg tilt)

Evolutions of pressure contours and free surface profiles

Several typical snapshots of pressure contours and free surface profiles for Case1 are shown as Fig.5. According to the Fig.5 (a~b), impact pressure occurs around the apex of wedge rapidly. Then, the high pressure region is divided into two zones and spreads along both sides of the wedge, as shown in Fig.5 (b~d). At the same time, the liquid spray jet formed and travels along the boundary of wedge. Since energy absorbed by motion of fluid particles, the maximum value of pressure decreases with the drop of the wedge.

Snapshots of pressure contours and free surface profiles for Case2 are shown as Fig.6. According to the Fig.6 (a~b), impact pressure also occurs around the apex of wedge firstly. However, the region of high pressure is asymmetric compared against that of Case1. Then, the high pressure region spreads along left side of the wedge, as shown in Fig.6 (b~d). As the wedge dropped into water with a tilting angle of 10deg, area of wet surface at the left side boundary is larger than that of the right side.

Snapshots of pressure contours and free surface profiles for Case3 are shown as Fig.7. Evolution of the high pressure zone is similar to that shown in Fig.6. However, the maximum value of pressure is much larger than that of Case2 compared at the same instant. Besides, area of wet surface at the left side boundary in Case3 increases faster than that of Case2.

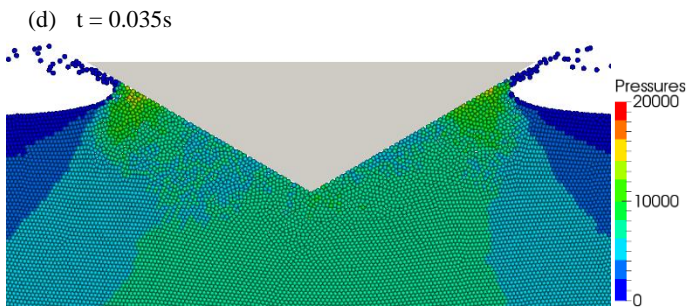
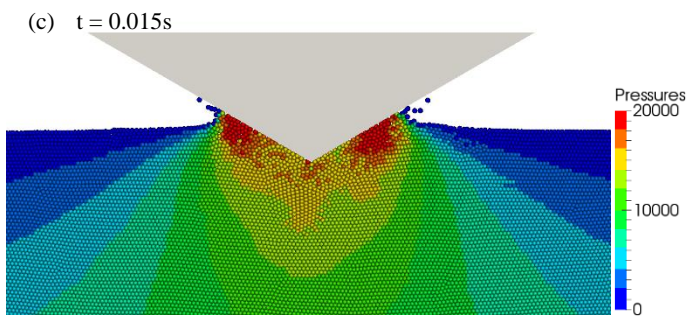
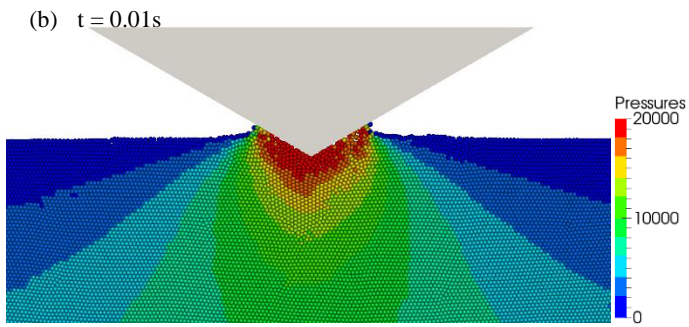
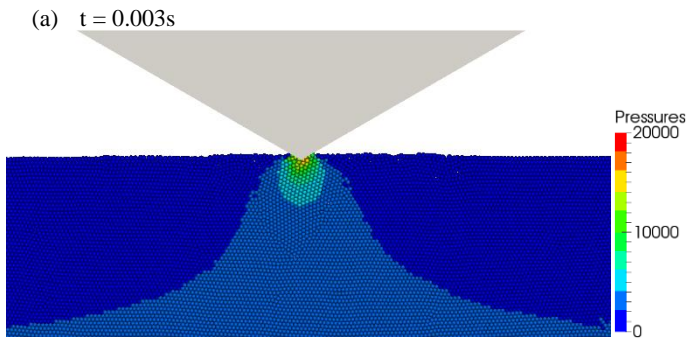


Fig.5 Snapshots of pressure contours and free surface profiles for Case1 (0deg tilt)

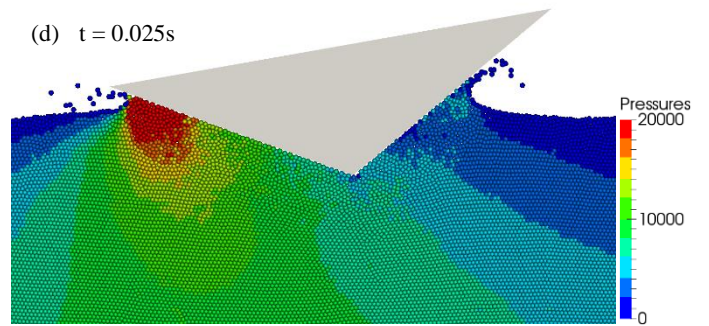
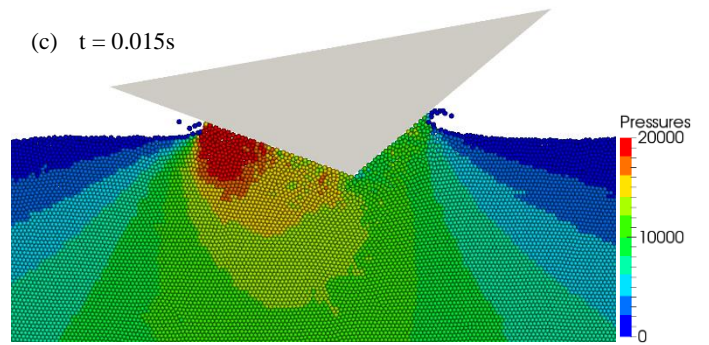
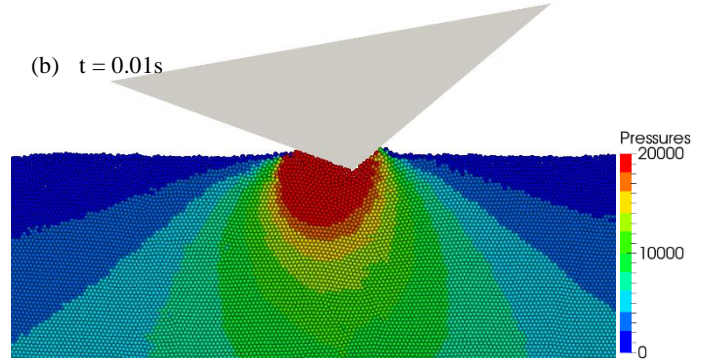
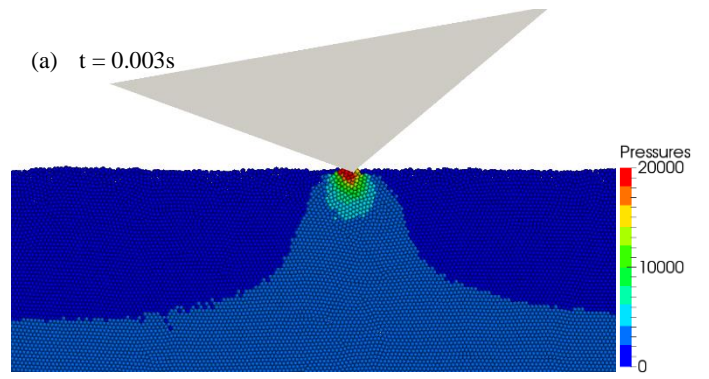


Fig.6 Snapshots of pressure contours and free surface profiles for Case2 (10deg tilt)

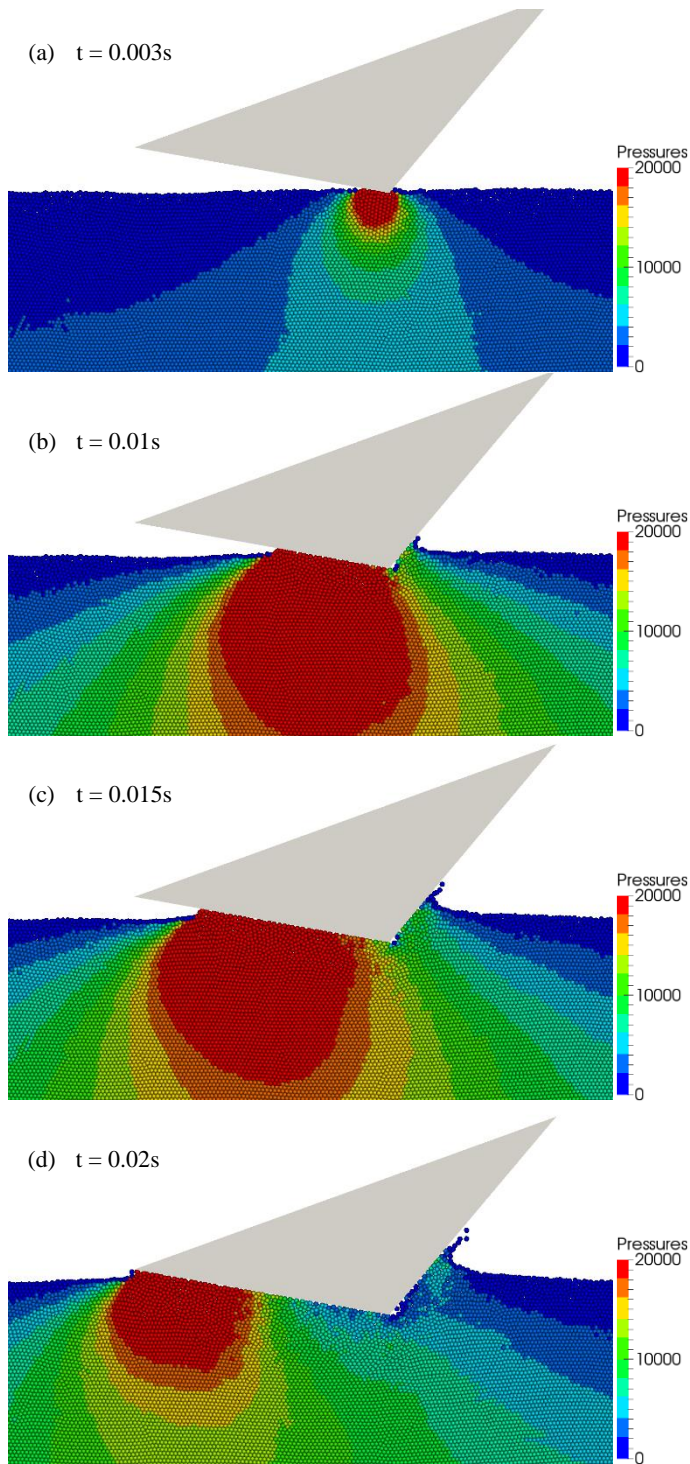


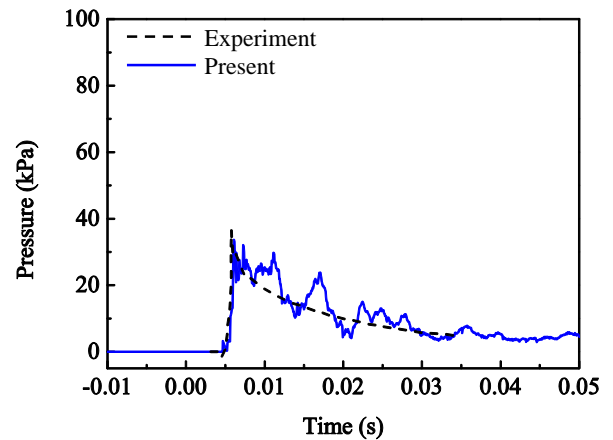
Fig.7 Snapshots of pressure contours and free surface profiles for Case3 (20deg tilt)

Time histories of impact pressures

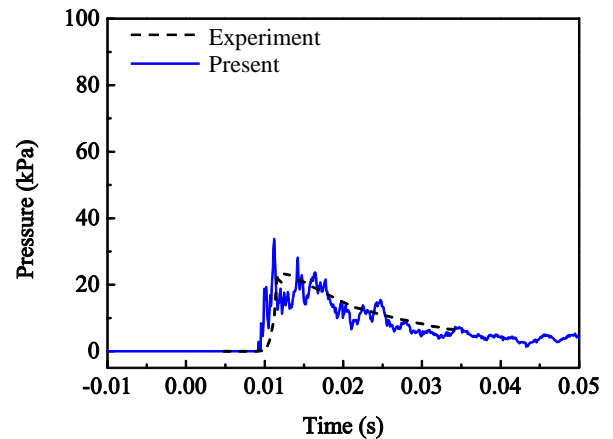
Time history of pressure for Case1 is shown as Fig.8. Numerical pressures of both sensors are compared against experimental data of the WILS JIP-III. According to Fig.8 (a), the impact pressure increases up to the peak value in a very short time. Though oscillation exists, time history of numerical pressure keeps with the trend of experimental data

at the location of sensor1. Similar situation occurs at the location of sensor2, and shown as Fig.8 (b). However, the peak value obtained by sensor2 is smaller than that of sensor1, and impact load is measured later at the location of sensor2.

For the cases of asymmetric wedge drop, time histories of pressures are shown as Fig.9 and Fig.10. Numerical results of wedges with tilting angle of 10deg and 20deg also coincide with the trend of experimental pressure data. Besides, peak values of impact pressures obtained by both sensors also increase with the enlargement of tilting angles. However, the peak values of wedge tilted 20deg are much larger than that of experimental results. According to the work by Lee et al. (2010), air-cushion effects on impact pressure cannot be neglected while structure dropping onto water with a small incident angle. So, errors of Case3 should be induced by the ignorance of air phase in present MPS solver.

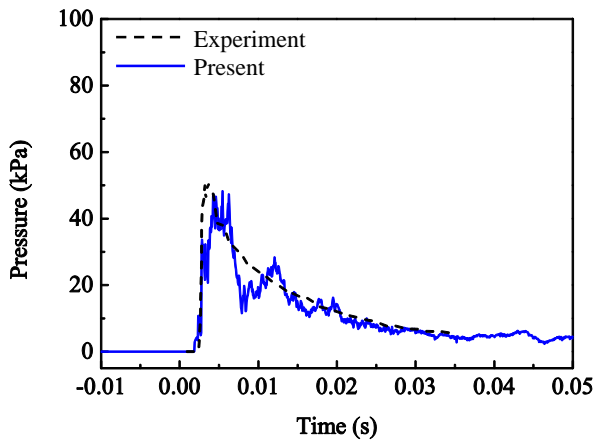


(a) Data of pressure sensor1

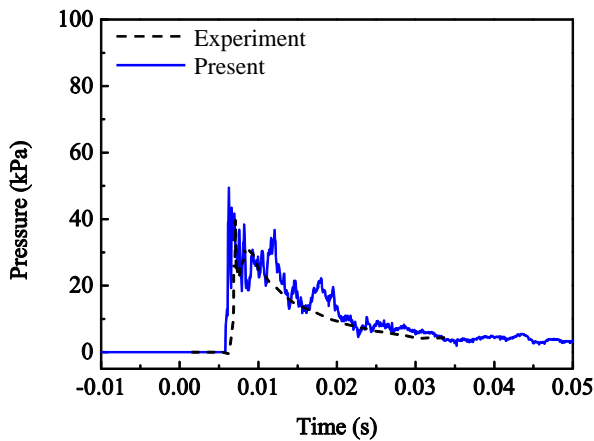


(b) Data of pressure sensor2

Fig.8 Comparison of pressures for Case1 (0deg tilt)



(a) Data of pressure sensor1



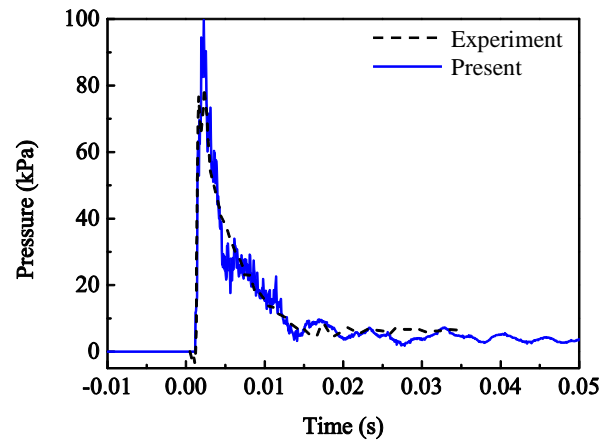
(b) Data of pressure sensor2

Fig.9 Comparison of pressures for Case2 (10deg tilt)

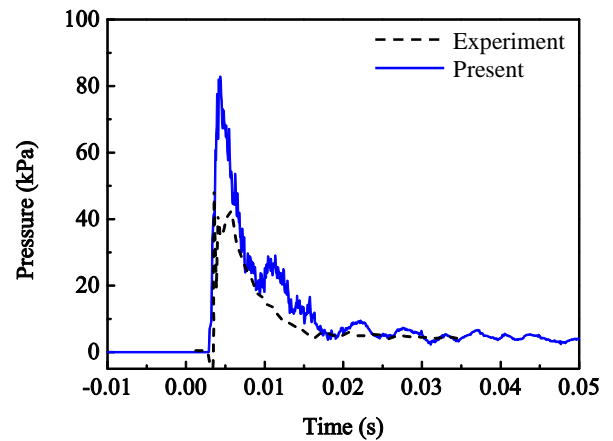
CONCLUSIONS

In this paper, water entry problem is numerically studied by the improved MPS method. To suppress the numerically unphysical pressure oscillation of traditional MPS method, several improvements are proposed. Then, symmetric and asymmetric wedge free-dropping tests are numerically studied and compared against experimental data proposed by MOERI as part of the WILS JIP-III. Based on the results of simulations, the following conclusions are made:

- Time histories of velocity of the wedge with different tilting angles are in good agreement with experimental results.
- Time histories of numerical pressures keep with the trend of experimental data. Peak values of impact pressures obtained by both sensors increase with the enlargement of tilting angles.



(a) Data of pressure sensor1



(b) Data of pressure sensor1

Fig.10 Comparison of pressures for Case3 (20deg tilt)

ACKNOWLEDGEMENTS

This work is supported by National Natural Science Foundation of China (Grant Nos. 51379125, 51490675, 11432009, 5141130131), High Technology of Marine Research Project of The Ministry of Industry and Information Technology of China, Chang Jiang Scholars Program (Grant No. T2014099), the Program for Professor of Special Appointment (Eastern Scholar) at Shanghai Institutions of Higher Learning (Grant No. 2013022), and foundation of State Key Laboratory of Ocean Engineering (Grant No. GKZD010065), to which the authors are most grateful.

REFERENCES

- Amicarelli, A, Albano, R, Mirauda, D, Agate, G, Sole, A, and Guandalini, R (2015). "A Smoothed Particle Hydrodynamics model for 3D solid body transport in free surface flows," *Computers & Fluids*, 116, 205-228.
- Hwang, SH, Khayyer, A, Gotoh, H, and Park, JC (2015). "Simulations of Incompressible Fluid Flow-Elastic Structure Interactions by a Coupled Fully Lagrangian Solver," *Proc 25th Int Offshore and Polar Eng Conf*, Hawaii, ISOPE, 1247-1250.

- Ikari, H, Khayyer, A, and Gotoh, H (2015). "Corrected higher order Laplacian for enhancement of pressure calculation by projection-based particle methods with applications in ocean engineering," *J Ocean Eng Mar Energy*, 1, 361-376.
- Khayyer, A, and Gotoh, H (2009). "Modified Moving Particle Semi-implicit methods for the prediction of 2D wave impact pressure," *Coastal Engineering*, 56, 419-440.
- Khayyer, A, and Gotoh, H (2010). "A higher order Laplacian model for enhancement and stabilization of pressure calculation by the MPS method," *Applied Ocean Research*, 32, 124-131.
- Khayyer, A, and Gotoh, H (2011). "Enhancement of stability and accuracy of the moving particle semi-implicit method," *Journal of Computational Physics*, 230, 3093-3118.
- Khayyer, A, and Gotoh, H (2012). "A 3D higher order Laplacian model for enhancement and stabilization of pressure calculation in 3D MPS-based simulations," *Applied Ocean Research*, 37, 120-126.
- Kim, KH, Lee, DY, Hong, SY, Kim, BW, Kim, YS, Nam, BW (2014). "Experimental Study on the Water Impact Load on Symmetric and Asymmetric Wedges," *Proc 24th Int Offshore and Polar Eng Conf*, Busan, ISOPE, 710-716.
- Kondo, M, and Koshizuka, S (2011). "Improvement of stability in moving particle semi-implicit method," *Int J Numer Meth Fluids*, 65, 638-654.
- Koshizuka, S, and Oka, Y (1996). "Moving-particle Semi-implicit Method for Fragmentation of Incompressible Fluid," *Nuclear Science and Engineering*, 123, 421-434.
- Koukouvinis, PK, Anagnostopoulos, JS, Papanonis, DE (2013). "Simulation of 2D wedge impacts on water using the SPH-ALE method," *Acta Mech*, 224, 2559-2575.
- Lee, BH, Park, JC, Kim, MH, Jung, SJ, Ryu, MC, and Kim, YS (2010). "Numerical simulation of impact loads using a particle method," *Ocean Engineering*, 37, 164-173.
- Lee, BH, Park, JC, Kim, MH, and Hwang, SC (2011). "Step-by-step improvement of MPS method in simulating violent free-surface motions and impact-loads," *Computer Methods in Applied Mechanics and Engineering*, 200, 1113-1125.
- Liu, H, Gong, K, and Wang, BL (2012). "Numerical Simulation of Violent Evolution of Free Surface during Water Entry of Wedge," *Proceedings of the Tenth Pacific/Asia Offshore Mechanics Symposium*, 153-156.
- Ma, L, and Liu, H (2014). "Two-Phase SPH Simulations of Wedge Water Entry," *Proceedings of the Eleventh Pacific/Asia Offshore Mechanics Symposium*, 218-224.
- Monaghan, JJ (1994). "Simulating free surface flows with SPH," *J Comput Phys*, 110, 399-406.
- Oger, G, Doring, M, Alessandrini, B, and Ferrant, P (2006). "Two-dimensional SPH simulations of wedge water entries," *Journal of Computational Physics*, 213, 803-822.
- Shao, SD (2009). "Incompressible SPH simulation of water entry of a free-falling object," *Int J Numer Meth Fluids*, 59:91-115.
- Southall, NR, Lee, YH, Johnson, MC, Hirdaris SE, and White, NJ (2014). "Towards a Pragmatic Method for Prediction of Whipping: Wedge Impact Simulations using OpenFOAM," *Proc 24th Int Offshore and Polar Eng Conf*, Busan, ISOPE, 806-815.
- Sun, Z, Xing, JT, Djidjeli, K, and Cheng, F (2015). "Coupling MPS and Modal Superposition Method for Flexible Wedge Dropping Simulation," *Proc 25th Int Offshore and Polar Eng Conf*, Hawaii, ISOPE, 144-151.
- Tanaka, M, and Masunaga, T (2010). "Stabilization and smoothing of pressure in MPS method by Quasi-Compressibility," *J Comp Phys*, 229, 4279-4290.
- Tang, ZY, and Wan, DC (2015). "Numerical simulation of impinging jet flows by modified MPS method," *Engineering Computations*, 32(4), 1153-1171.
- Von Karman, T (1929). "The impact on seaplane floats during landing," National Advisory Committee for Aeronautics, TN-321.
- Wagner, H (1932). "Uber stoss-und Gleitvorgange ander Oberflache von Flussikeiten," *Zeitschr F Angew Math Und Mech*, 12(4), 193-235.
- Yang, QY, Qiu, W (2012). "Numerical simulation of water impact for 2D and 3D bodies," *Ocean Engineering*, 43, 82-89.
- Yokoyama, M, Kubota, Y, Kikuchi, K, Yagawa, G, and Mochizuki, O (2014). "Some remarks on surface conditions of solid body plunging into water with particle method," *Advanced Modeling and Simulation in Engineering Sciences*, 1:9.
- Zhang, Y X, and Wan, DC (2011). "Application of MPS in 3D Dam Breaking Flows," *Sci Sin Phys Mech Astron*, 41, 140-154.
- Zhang, YX, and Wan, DC (2012). "Apply MPS Method to Simulate Liquid Sloshing in LNG Tank," *Proc 22nd Int Offshore and Polar Eng Conf*, Rhodes, Greece, 381-391.
- Zhang, YX, Wan, DC, Hino, T (2014). "Comparative study of MPS method and level-set method for sloshing flows," *Journal of hydrodynamics*, 26(4), 577-585.